DOI: 10.1002/chem.200902011

Tetraamine-Derived Bifunctional Chelators for Technetium-99m Labelling: Synthesis, Bioconjugation and Evaluation as Targeted SPECT Imaging Probes for GRP-Receptor-Positive Tumours**

Keelara Abiraj,[a] Rosalba Mansi,[a] Maria-Luisa Tamma,[a] Flavio Forrer,[b] Renzo Cescato,[c] Jean Claude Reubi,[c] Kayhan G. Akyel,[d] and Helmut R. Maecke*[a, e]

Abstract: Owing to its optimal nuclear properties, ready availability, low cost and favourable dosimetry, ^{99m}Tc continues to be the ideal radioisotope for medical-imaging applications. Bifunctional chelators based on a tetraamine framework exhibit facile complexation with $Tc(V)O_2$ to form monocationic species with high in vivo stability and significant hydrophilicity, which leads to favourable pharmacokinetics. The synthesis of a series of 1,4,8,11-tetraazaundecane derivatives (**01**–**06**) containing different functional groups at the 6-position for the conjugation of biomolecules and subsequent labelling with ^{99m}Tc is described herein. The chelator **01** was used as a starting material for the facile synthesis of chelators functionalised with OH (**02**), N_3 (**04**) and *O*-succinyl ester (**05**) groups. A straightforward and easy synthesis of carboxyl-functionalised tetraamine-based chelator **06** was achieved by using inexpensive and commercially available starting materials. Conjugation of **06** to a potent bombesin-antagonist peptide and subsequent labelling with ^{99m}Tc afforded the radiotracer ^{99m}Tc-N4-BB-ANT, with radiolabelling yields of >97% at a specific activity of 37 GBq μmol^{-1}. An IC_{50} value of (3.7±1.3) nM was obtained, which confirmed the high affinity of the conjugate to the gastrin-releasing-peptide receptor (GRPr). Immunofluorescence and calcium mobilisation assays confirmed the strong antagonist properties of the conjugate. In vivo pharmacokinetic studies of ^{99m}Tc-N4-BB-ANT showed high and specific uptake in PC3 xenografts and in other GRPr-positive organs. The tumour uptake was (22.5±2.6)% injected activity per gram (% IA g^{-1}) at 1 h post injection (p.i.). and increased to (29.9±4.0)% IA g^{-1} at 4 h p.i. The SPECT/computed tomography (CT) images showed high tumour uptake, clear background and negligible radioactivity in the abdomen. The promising preclinical results of ^{99m}Tc-N4-BB-ANT warrant its potential candidature for clinical translation.

Keywords: antitumor agents · bifunctional chelators · imaging agents · radiopharmaceuticals · technetium

Introduction

Despite the growing importance of ^{18}F-labelled innovative radiopharmaceuticals for positron emission tomography (PET)[1] and the availability of hybrid instruments such as PET/CT, the use of gamma emitters, mostly radiometals, is still essential for SPECT and SPECT/CT studies.[2] The working horse of the nuclear-medicine physician continues

[a] Dr. K. Abiraj, Dr. R. Mansi, M.-L. Tamma, Prof. H. R. Maecke
Division of Radiological Chemistry
University Hospital of Basel, 4031 Basel (Switzerland)
Fax: (+41) 61-265-4699
E-mail: hmaecke@uhbs.ch

[b] Dr. F. Forrer
Institute of Nuclear Medicine
University Hospital of Basel, 4031 Basel (Switzerland)

[c] Dr. R. Cescato, Prof. J. C. Reubi
Division of Cell Biology and Experimental Cancer Research
Institute of Pathology
University of Berne, Murtenstrasse 31, 3010 Berne (Switzerland)

[d] K. G. Akyel
Novartis Institutes for BioMedical Research
4002 Basel (Switzerland)

[e] Prof. H. R. Maecke
Current Address:
Department of Nuclear Medicine
University of Freiburg, Hugstetterstrasse 55
79106 Freiburg (Germany)
Fax: (+49) 761-270-3930
E-mail: helmut.maecke@uniklinik-freiburg.de

[**] SPECT: single-photon-emission computed tomography; GRP: gastrin-releasing peptide.

to be ^{99m}Tc. ^{99m}Tc is preferred due to its favourable γ energy (141 keV), suitable half life of 6 h, which minimises the dose to the patient, availability through a generator, cost effectiveness and well-established chemistry. A variety of ^{99m}Tc-bifunctional chelators for coupling to bioactive molecules such as peptides and proteins have therefore been developed and evaluated. These chelators stabilise different oxidation states of the Tc atom. The most popular and suitable labelling strategy is the indirect or postconjugation labelling approach. The aim is to couple a bifunctional chelating agent (BFCA) to the biomolecule without loss of biological potency and possibly to be able to provide it as a freeze-dried kit formulation. At the time of application, labelling is performed by adding generator-produced $^{99m}TcO_4^-$.

Different labelling strategies have been developed over the years. Recently, the focus has been the use of the versatile *fac*-$[^{99m}Tc(CO)_3(H_2O)_3]^+$ core.[3] In this complex, the metal has the d^6-Tc^I low-spin electron configuration, which confers high kinetic stability to metal complexes. Fortunately, the facially coordinated water molecules exchange rapidly with a variety of tridentate chelators to allow fast and efficient labelling of biomolecules at relatively low concentrations. These Tc complexes show octahedral geometry; examples are N^{α}-carboxymethylhistidine (N^{α}Hisac) coupled to bombesin[4] and neurotensin.[5]

The ^{99m}Tc-HYNIC core was also employed for the labelling of antibodies,[6] chemotactic peptides,[7,8] somatostatin[9] and gastrin analogues.[10] HYNIC stands for 6-hydrazinonicotinic acid; the carboxylic acid group was used for coupling to the N-terminal amine group of peptides. HYNIC may act as a mono- or bidentate ligand and needs co-ligands such as tricine or *N*,*N*′-ethylenediaminediacetic acid to complete the coordination polyhedron. HYNIC was successfully coupled to [Tyr^3]octreotide (TOC) or [Tyr^3,Thr^8]octreotide (TATE).[11] Kit-based formulations were developed that could be labelled very efficiently.[12] Clinical studies have proven high diagnostic sensitivity and utility in daily clinical practice without the need for sophisticated radiopharmacy.[13,14]

Nevertheless, there are uncertainties with HYNIC-labelled biomolecules concerning the homogeneity of the radiopharmaceuticals with regard to the coordination mode of the HYNIC ligand (different isomers were shown by using HPLC–MS).[9]

Tetradentate chelators forming square-pyramidal Tc complexes with the $[Tc{=}O]^{3+}$ core are most frequently used. Examples are bifunctional derivatives of propylenediaminedioxime (PnAO) based chelators (for example, 6-*p*-isothiocyanatobenzyl-3,3,9,9-tetramethyl-4,8-diazaundecane-2,10-dione dioxate) coupled to octreotide[15] and biotin.[16] In addition, N_3S (triamide thiols),[17–19] N_2S_2 (diamidedithiols, DADS),[19,20] N_2S_2 (monoamidemonoaminedithiols, MAMA)[19,21,22] and N_2S_2 (diaminedithiols)[23–26] chelators were coupled to different biomolecules for ^{99m}Tc labelling. Overall, this group of BFCAs is the most frequently used.

Finally, the $[O{=}Tc{=}O]^+$ core, which forms octahedral Tc complexes with linear or macrocyclic tetraamines such as bifunctional cyclam-14[27] and bifunctional 1,4,8,11-tetraazaundecane,[28–31] has been coupled to bioactive peptides as well as to biotin.[32] The monocationic unit $[Tc(V)O_2](tetraamine)^+$ shows high kinetic stability and confers high hydrophilicity to the peptides studied so far. In particular, when this approach was applied to somatostatin, gastrin and bombesin analogues, highly favourable pharmacokinetics were reported in animal models[28–31] and human patients.[33,34]

Despite this success, tetraamine-based conjugates have not found widespread use. We assume that this is due to the lack of synthesis protocols and the rather tedious multistep synthesis of some of the N_4-based synthons. Therefore, we have set out a programme for the synthesis of 1,4,8,11-tetraazaundecane derivatives with different functional groups in the 6-position (Scheme 1) to allow a variety of bioconjugation strategies, such as peptide amide formation in solid-phase peptide synthesis (X = COOH), click chemistry (X = N_3), ester formation (X = OH) or reaction with the C terminus of a peptide or protein (X = NH_2). The synthesis and characterisation of these prochelators are described in this manuscript. In addition, we report one example of the solid-phase peptide synthesis of a bombesin-based receptor antagonist modified with a glycine-4-aminobenzoyl spacer[35] and coupled to 6-carboxy-1,4,8,11-tetraazaundecane. A full in vitro and in vivo (PC3 prostate tumour xenograft-bearing mice) characterisation of the ^{99m}Tc-labelled peptide is presented, including measurement of the antagonist potency by using immunofluorescence and Ca^{2+}-flux measurements.

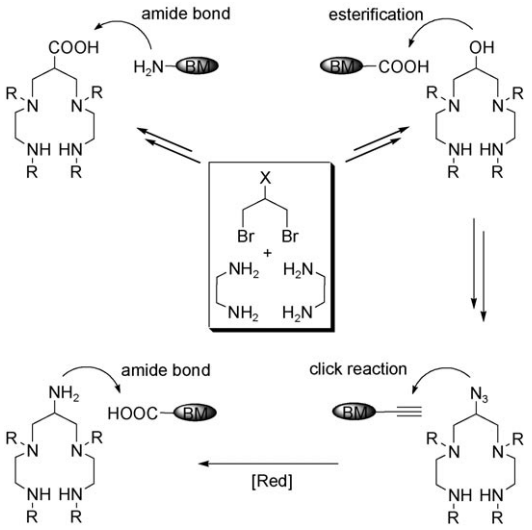

Scheme 1. Illustration of various tetraamine-derived bifunctional chelators for conjugation of vector biomolecule and subsequent labelling with ^{99m}Tc. X: OH or COOH; R: protecting group; BM: biomolecule.

Bombesin receptors are of major interest in the development of targeted agents for molecular imaging and radionuclide therapy of major human cancers. In particular, the bombesin receptor 2 (BB2 or gastrin-releasing-peptide

(GRP) receptor) was shown to be overexpressed in prostate cancer, breast cancer, small-cell lung cancer and gastrointestinal stromal tumours.[36] We have focused on antagonists in this work because they may be superior to agonists for in vivo receptor imaging.[37,38]

Results and Discussion

^{99m}Tc is still the most important radionuclide in molecular-imaging studies with nuclear probes. In addition, it is leading the way for agents useful in targeted radionuclide therapy because it shares many chemical coordination properties with the high-energy β-emitters ^{186}Re and ^{188}Re.

Design and synthesis of bifunctional chelators: Scheme 1 illustrates the design of various tetraamine-based bifunctional chelators, which are accessible in a few synthetic steps from inexpensive and commercially available materials. Different functional groups, such as COOH, OH, O–$(CH_2)_2$COOH, N_3 or NH_2, at the 6-position allow facile conjugation of the biomolecule by using suitable coupling or ligation methods. The carboxyl-functionalised tetraamine chelator is ideal for the coupling of biomolecules either on a solid or in the solution phase through conventional amide-bond formation. The synthesis of a hydroxy-functionalised chelator is of particular interest because it can be employed for the conjugation of a biomolecule or any other functionalised synthon by esterification. It can also be used for the introduction of a linker between the chelate and the pharmacophore part of the molecule. Furthermore, it is a useful precursor for the facile synthesis of tetraamine chelators bearing an azide group.

In recent years, the Cu^I-catalysed azide–alkyne cycloaddition, often referred to as click chemistry, has been of immense interest for bioconjugation reactions.[39,40] Developed by Sharpless and co-workers[41] and by Meldal and colleagues,[42] this ligation reaction forming a triazole from an azide and a terminal alkyne is characterised by its unprecedented selectivity and coupling efficiency under mild conditions. In this context, the azide-functionalised tetraamine-based chelator would be of great interest for selective conjugation to the terminal alkyne of a biomolecule containing other unprotected reactive functionalities. In addition, the reduction of the azide group affords an amino-functionalised bifunctional chelator, which is also a potential precursor for bioconjugation.

The overall synthetic approach, whereby the different tetraamine-based bifunctional chelators are synthesised for conjugation to a biomolecule and subsequent labelling with ^{99m}Tc, is presented in Scheme 2. The synthesis of the hydroxy-functionalised chelator **02** is started with monoalkylation of ethylenediamine (large excess) by using 1,3-dibromo-2-propanol. The intermediate tetraamine, **01**, was isolated as a tetrahydrochloride salt in pure form. The successive introduction of Boc protecting groups to **01** yielded the required prochelator **02** in 86% yield.

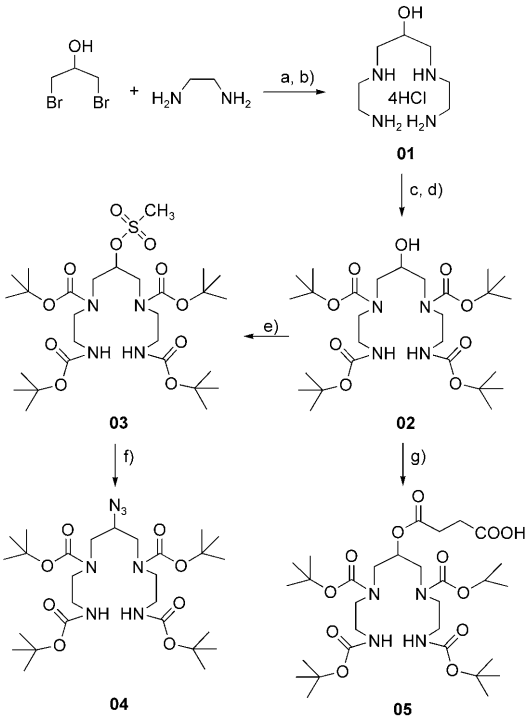

Scheme 2. Synthesis of tetraamine-derived bifunctional chelators: a) 110°C, 24 h; b) 12 M HCl, EtOH, H_2O, 72%; c) ion-exchange chromatography, 94%; d) $(Boc)_2O$, DIPEA, DMF, 86%; e) CH_3SO_2Cl, pyridine, 82%; f) NaN_3, DMF, 75°C, 88%; g) succinic anhydride, DMAP, THF, 92%. Boc: *tert*-butoxycarbonyl; DIPEA: *N*,*N*-diisopropylethylamine; DMF: *N*,*N*-dimethylformamide; DMAP: 4-dimethylaminopyridine; THF: tetrahydrofuran.

The azido-functionalised chelator **04** was obtained from **02** in a two-step reaction with an overall yield of 72%. Mesylation of **02** with methylsulfonyl chloride and pyridine yielded the intermediate **03** in 82% yield; this compound was further treated with sodium azide to get the desired bifunctional chelator **04** in 88% yield after chromatographic purification. This is an elegant route for the facile synthesis of the azido-functionalised tetraamine-based chelator in a few steps. Precursor **02** was further subjected to esterification with succinic anhydride to obtain the carboxyl-functionalised chelator **05** in high yield (92%). This strategy is advantageous if a spacer is needed to separate the biomolecule from the chelator.

The carboxyl-functionalised chelators are compatible with solid-phase peptide synthesis and are highly desirable for the vectorisation of small peptidyl ligands. They can be introduced directly to the N terminus of the bioactive peptide after assembly of the desired amino acids on the solid phase. Hence, our efforts were devoted toward the development of a simple and straightforward method for the synthesis of a carboxyl-functionalised tetraamine chelator. As a result, we synthesised prochelator **06** in a 'one-pot' procedure by the reaction of commercially available 3-bromo-2-(bromomethyl)propionic acid with a high excess of ethylenediamine (Scheme 3). The excess of solvent and ethylenediamine were removed by evaporation under reduced pressure and

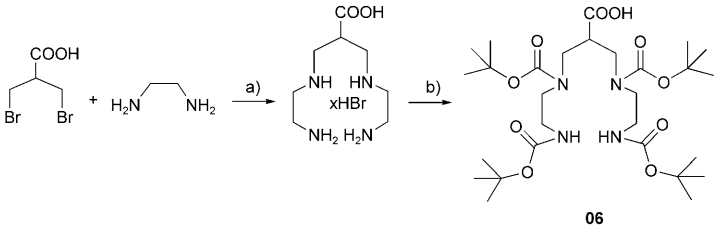

Scheme 3. Straightforward synthesis of carboxyl-functionalised tetraamine-based bifunctional chelator **06**: a) THF, RT; b) $(Boc)_2O$, 1 N NaOH, dioxane/H_2O, 4 °C to RT, 1 h, 62 %.

the resulting intermediate was subjected to Boc protection without any further purification. Chelator **06** was obtained in an overall yield of 62 % after purification by column chromatography.

Peptide conjugation and radiolabelling: To validate the utility of the synthesised bifunctional chelators, we chose a bombesin-antagonist peptide for bioconjugation. The peptide (D-Phe-Gln-Trp-Ala-Val-Gly-His-Sta-Leu-NH_2; Sta: statine) was synthesised on the solid phase by assembling the desired amino acids and a glycine-4-aminobenzoyl spacer was introduced. The carboxyl-functionalised prochelator **06** was easily coupled to the N terminus of the peptide on the solid phase by using N-[(dimethylamino)-1*H*-1,2,3-triazole-[4,5-*b*]-pyridin-1-ylmethylene]-*N*-methylmethanaminium hexafluorophosphate (HATU) as the activating agent. Cleavage from the resin followed by deprotection and reversed-phase (RP) HPLC purification afforded the conjugate N4-BB-ANT in >97 % purity (Scheme 4). The conjugate was characterised by using analytical RP-HPLC and ESI-MS.

The conjugate was labelled with ^{99m}Tc in phosphate buffer (pH 11.5) by using $^{99m}TcO_4^-$ generator eluate. Tin(II) chloride was used as the reducing agent, with citrate anions as an intermediate-supporting Tc(V) ligand. The labelling was

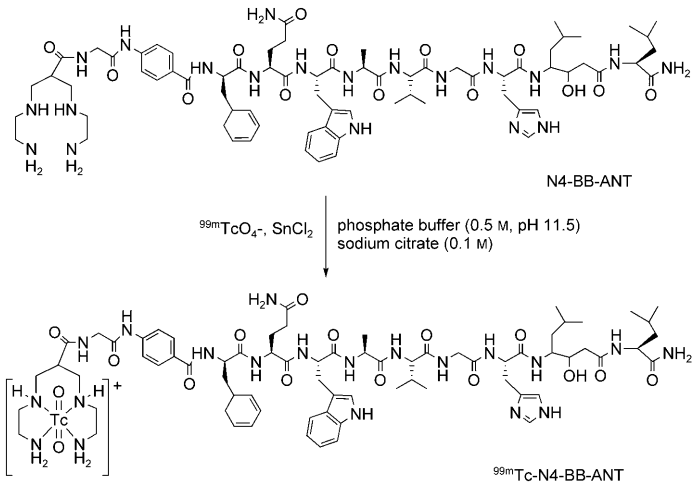

Scheme 4. Structure of the tetraamine-conjugated bombesin antagonist and radiolabelling with ^{99m}Tc.

completed within 30 min at room temperature and resulted in ^{99m}Tc-N4-BB-ANT with radiolabelling yields of >97 % at a specific activity of 37 GBq μmol^{-1}. The quality control performed by using analytical RP-HPLC showed the presence of a minute amount of radiochemical impurities (<3 %) due to the formation of expected impurities such as [^{99m}Tc]citrate, $^{99m}TcO_2 \cdot x\,H_2O$ and unlabelled $^{99m}TcO_4^-$.

Receptor binding affinity: Table 1 lists the IC_{50} values of N4-BB-ANT, RM1, a DOTA-conjugated peptide that we identified previously as potent bombesin antagonist,[38] and the antagonist BIM26226.[43] N4-BB-ANT shows the highest affinity of the three peptides for the GRP receptors; the values for the two chelator-conjugated peptides, N4-BB-ANT and RM1, differ by 10-fold. This correlates with data that we obtained earlier indicating that positive charges at the N terminus of bombesin(7–14)-based agonists distinctly increase binding affinity to the GRP receptor.[44]

Table 1. In vitro GRP-receptor binding affinities (IC_{50}) and calcium-mobilisation inhibition values (EC_{50}) of bombesin antagonists.

Compound	Sequence[a]	IC_{50}[b] [nM]	EC_{50}[b] [nM]
N4-BB-ANT	N4-*X*-D-Phe-Gln-Trp-Ala-Val-Gly-His-Sta-Leu-NH_2	3.7 ± 1.3	0.28 ± 0.1
RM1	DOTA-*X*-D-Phe-Gln-Trp-Ala-Val-Gly-His-Sta-Leu-NH_2	35 ± 9.0	2.89 ± 1.2
BIM26226	D-F_5-Phe-Gln-Trp-Ala-Val-D-Ala-His-Leu-OMe	13.5 ± 0.5	0.75 ± 0.2

[a] *X*: Gly-4-aminobenzoyl; DOTA: 1,4,7,10-tetraazacyclododecane-1,4,7,10-tetraacetic acid. [b] Values represent the mean ± SEM of $n \geq 3$ experiments.

Immunofluorescence-based internalisation assay: An immunofluorescence-based internalisation assay was performed by using HEK-GRPr cells to assess the antagonist properties of N4-BB-ANT (Figure 1). Massive internalisation of GRP receptors into the cells was induced when they were treated with 10 nmol L^{-1} of bombesin. Conversely, the receptors are localised on the cell surface in the absence of peptide and also when incubated with 1 μmol L^{-1} of N4-BB-ANT. Thus, unlike the typical agonist, N4-BB-ANT failed to induce massive internalisation of GRP receptors and showed antagonist properties. However, at a concentration of 1 μmol L^{-1} and together with 10 nmol L^{-1} of bombesin, N4-BB-ANT was able to antagonise bombesin-induced receptor internalisation.

Calcium-mobilisation assay: The antagonist potency of N4-BB-ANT was further evaluated by using a calcium-mobilisation assay in PC3 cells. Figure 2 illustrates the efficacy of N4-BB-ANT for inhibition of intracellular calcium mobilisation stimulated by the agonist Tyr^4–bombesin, in comparison with potent antagonists RM1 and BIM26226. Addition of Tyr^4–bombesin (100 nmol L^{-1}) induces maximum calcium mobilisation, which decreases with an increase in the concentration of the antagonists. At a concentration of

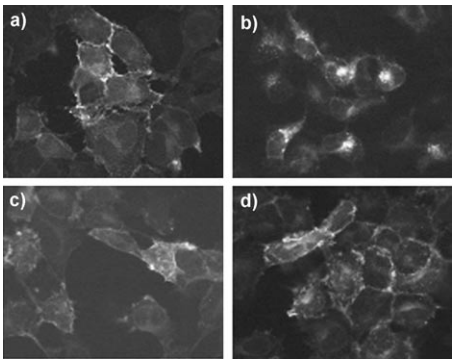

Figure 1. Immunofluorescence microscopy-based internalisation assay with HEK-GRPr cells showing that the GRP-receptor internalisation induced by bombesin is efficiently antagonised by N4-BB-ANT. a) Control experiment showing membrane-bound GRP receptors in the absence of peptide. b) Bombesin agonist (10 nmol L^{-1}) triggers massive GRP-receptor internalisation. c) N4-BB-ANT failed to induce GRP-receptor internalisation, even at a concentration of 1 μmol L^{-1}. d) The antagonist N4-BB-ANT (1 μmol L^{-1}) efficiently blocked the bombesin-agonist-mediated GRP-receptor internalisation.

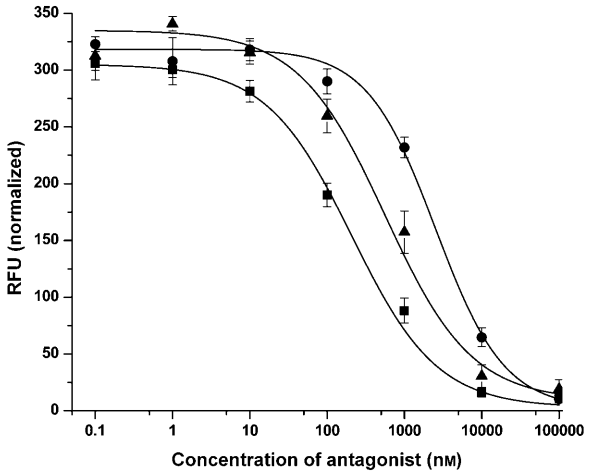

Figure 2. Representative inhibition curves of bombesin antagonists obtained by the calcium-release assay in PC3 cells (RFU: relative fluorescence unit). Cells were loaded with Ca dye and different concentrations of antagonists ranging from 0.1 nM to 100 μM. The curves show the potential of N4-BB-ANT (■), RM1 (●) and BIM26226 (▲) to inhibit the intracellular calcium mobilisation stimulated by the addition of the agonist Tyr^4-bombesin (100 nM).

>10 μmol L^{-1}, all of the antagonists completely inhibited the Tyr^4–bombesin-induced calcium mobilisation. Compared to the results for RM1 and BIM26226, N4-BB-ANT showed superior antagonist potency by shifting the inhibition curve to a lower concentration range. Consequently, N4-BB-ANT showed a 10-fold lower EC_{50} value than that of RM1, which is in accordance with their binding affinities to GRP receptors (Table 1).

Receptor-mediated cellular-uptake kinetics: Figure 3 shows the cellular-uptake kinetics of ^{99m}Tc-N4-BB-ANT. The radioligand showed high and specific uptake in PC3 cells. Blocking studies performed by using a large excess of cold antagonist peptide demonstrated that the uptake was receptor mediated. The radioligand showed rapid binding to the membrane receptors and the specific bound fraction levelled off at 40% within 2 h of incubation. The specific internalised fraction was about 10% and increased very slowly. This behaviour is contrary to that of agonists, which usually mediate rapid internalisation of the receptor–ligand complex and result in high amounts of internalised peptide and low amounts of bound peptide.

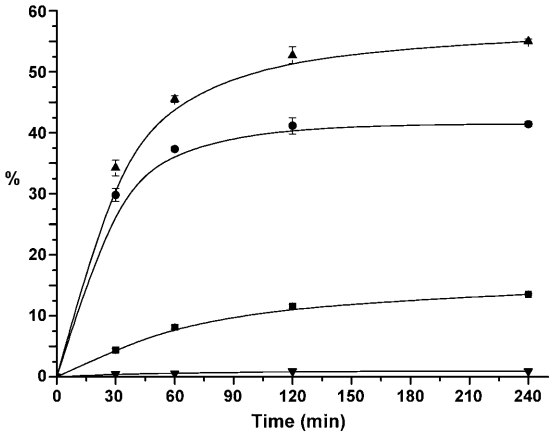

Figure 3. Cellular-uptake profile of ^{99m}Tc-N4-BB-ANT as measured with PC3 cells. Cells were incubated with the radioligand (0.25 pmol $well^{-1}$) at 37 °C and 5% CO_2 and the kinetics of uptake were analysed at different time points. The percentage of the specific bound (●), specific internalised (■) and total specific (▲) cell uptake was determined with respect to the total added activity. The non-specific uptake (▼) was determined by pre-treating the cells with a 1000-fold excess of blocking agent (BIM26226) before addition of the radioligand. Values and standard deviations are the result of two independent experiments with triplicates of each experiment.

The fate of GRPr-bound ^{99m}Tc-N4-BB-ANT: Radiolabelled agonists of regulatory peptides usually internalise upon binding to and activation of G-protein-coupled receptors, whereas antagonists stay bound to the receptor. We studied the fate of receptor-bound ^{99m}Tc-N4-BB-ANT by using a temperature-shift experiment. The radiopeptide was allowed to bind at 4 °C and then the concentrations on the cell surface, in the cell medium and in the cytoplasm (internalised) were determined upon a temperature shift to 37 °C. Figure 4 summarises the kinetics of the different pathways. The medium is devoid of free radiopeptide at the start of the experiment. The disappearance from the cell surface follows pseudo-first-order kinetics with the observed rate (k_{obs}) = the rate of disappearance (k_{dis}) = the sum of the rates of dissociation and internalisation ($k_{off}+k_{int}$) $=2.42\times10^{-2}$ min^{-1} ($t_{1/2}=$ 28.6 min). The data indicate that there is a fast pseudo-first-order disappearance of the radioligand from the cell surface, which almost reaches a steady state after 3–4 h. Surprisingly, there is a relatively fast internalisation of almost 20% of the surface-bound peptide within about 30 min. This is unusual because most antagonists do not internalise or initiate inter-

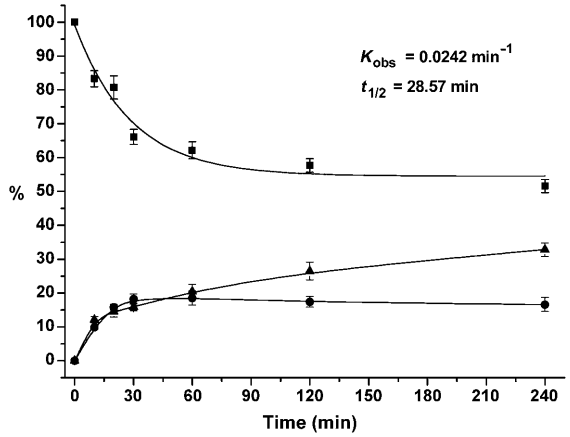

Figure 4. Fate of the receptor-bound ^{99m}Tc-N4-BB-ANT as measured with PC3 cells. The radioligand (0.25 pmol well^{-1}) was allowed to bind to the GRP receptors on PC3 cells at 4 °C. After 2 h, the medium was removed and the fate of the receptor-bound radioligand was studied by adding fresh medium and incubating the cells at 37 °C and 5% CO_2. The percentage of bound (■),internalised (●) and dissociated (▲) radioligand was measured with respect to the total receptor-bound radioligand over a period of 2 h at 4 °C (100%). Values and standard deviations are the result of two independent experiments with triplicates of each experiment.

nalisation of the receptor–ligand complex. The observed internalisation is specific, as shown by a blocking experiment.

Biodistribution and imaging studies: We studied the pharmacokinetics of ^{99m}Tc-N4-BB-ANT in human PC3 xenograft-bearing nude mice at times 1, 4 and 24 h after injection. The results are given in Table 2. The radiopeptide showed reasonably fast clearance from the circulation. Only (0.4 ± 0.05) % IA g^{-1} was left after 4 h. The uptake in the PC3 tumour was very high and increased from (22.5 ± 2.6) % IA g^{-1} after 1 h to (29.91 ± 4) % IA g^{-1} after 4 h. After 24 h, the uptake was still (15.16 ± 0.95) % IA g^{-1}. The specificity to tumour and abdominal GRP-receptor-positive organs was shown by co- or preinjecting a 2000-fold excess of cold peptide. 95% of the uptake by the tumour and pancreas was blocked, whereas the uptake in the intestines and stomach was blocked by 88% and 82%, respectively.

Rapid and very high uptake in the pancreas and other GRP-receptor-expressing organs, such as the intestine, was also found. Unlike the situation with agonist-based radiopeptides, the antagonist ^{99m}Tc-N4-BB-ANT washes out from these abdominal organs rather quickly, which results in good tumour-to-non-tumour tissue ratios at early time points, as can be seen from the SPECT/CT study (Figure 5) and the data in Table 2. The images (coronal and transaxial) show a clear delineation of the tumour, low abdominal uptake and blocking of all GRP-receptor-positive organs upon preinjection of a large excess of cold peptide. The kidneys, which are the main organ of excretion, are faintly visible in the 12 h image. For good image contrast, absolute target uptake is important but a high target-to-non-target ratio is also mandatory. As seen from the data in Table 2, the tumour-to-blood ratio is high and increases with time. The pharmacokinetics profile of ^{99m}Tc-N4-BB-ANT is similar to the one of [^{99m}Tc]-Demobesin 1.[28] The higher tumour uptake and slower washout from the tumour mean that the tumour-to-normal-organ ratios of ^{99m}Tc-N4-BB-ANT are superior. In particular, the tumour-to-kidney ratio of 10.7 at 24 h appears to be the highest of any radiolabelled peptide described so far.

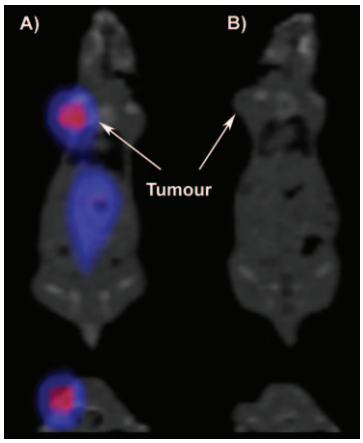

Figure 5. SPECT/CT images of PC3 tumour-bearing nude mice 12 h after injection of ^{99m}Tc-N4-BB-ANT. A) SPECT/CT coronal and transaxial image slices showing specific tumour uptake of ^{99m}Tc-N4-BB-ANT. B) SPECT/CT coronal and transaxial image slices showing blocking of ^{99m}Tc-N4-BB-ANT uptake in receptor-positive organs and tumour.

Table 2. Biodistribution of ^{99m}Tc-N4-BB-ANT in human PC3 xenograft-bearing nude mice at 1, 4 and 24 h after injection. Data are expressed as the percentage of injected activity per gram of tissue [% IA g^{-1}] and are presented as the mean ± SD (n = 4–6).

Organ	1 h	4 h	4 h blocked[a]	24 h
blood	1.69 ± 0.14	0.40 ± 0.05	0.24 ± 0.03	0.09 ± 0.02
tumour	22.50 ± 2.62	29.91 ± 4.00	1.66 ± 0.22	15.16 ± 0.95
kidneys	10.50 ± 1.20	6.12 ± 1.17	4.20 ± 1.87	1.42 ± 0.13
pancreas	64.86 ± 6.72	19.86 ± 2.35	1.05 ± 0.14	0.57 ± 0.21
muscle	0.43 ± 0.16	0.08 ± 0.02	0.07 ± 0.01	0.07 ± 0.01
intestine	6.97 ± 1.57	2.12 ± 0.37	0.26 ± 0.04	0.12 ± 0.01
liver	12.32 ± 1.01	7.75 ± 0.62	2.21 ± 0.32	3.88 ± 0.40
stomach	5.68 ± 0.01	4.86 ± 1.04	0.87 ± 0.11	0.42 ± 0.15
bone	1.34 ± 0.26	0.57 ± 0.11	0.36 ± 0.08	0.41 ± 0.19
Tumour-to-normal-tissue ratios				
tumour:blood	13.3	74.7		168
tumour:kidney	2.14	4.89		10.7
tumour:muscle	52.3	137		216
tumour:liver	1.83	3.86		3.91
tumour:intestine	3.23	14.0		126

[a] Blocked with N4-BB-ANT (20 nmoles).

The data indicate that the choice of chelator, including the corresponding $Tc(O)_2^+$ complex, distinctly changes the potency of this peptidic antagonist. If compared to recently reported data in the same animal model with the DOTA-conjugated and ^{111}In-labelled RM1,[38] ^{99m}Tc-N4-BB-ANT has superior properties due to higher receptor affinity and improved pharmacokinetics. The tumour uptake is distinctly

higher at each time point. Concomitantly, the tumour-to-normal-tissue ratios are higher as well.

Conclusions

In this manuscript, we have described the design, synthesis and characterisation of different acyclic tetraamine-based synthons (1,4,8,11-tetraazaundecane) with functional groups in the 6-position for facile conjugation to different functionalities of biomolecules. As an example, we described the solid-phase coupling of one of the N_4-synthons to a bombesin-based antagonist and ^{99m}Tc-labelling. The resulting radiopeptide was systematically evaluated in vitro and in vivo as a targeted imaging probe (SPECT, SPECT/CT).

This study resulted in the development of a new and clinically relevant GRP-receptor-binding peptide, N4-BB-ANT, which can be labelled with ^{99m}Tc at a high specific activity that is stable in vivo. The conjugate shows very promising pharmacokinetics and is a potential candidate for further clinical development as a targeted SPECT (SPECT/CT) agent for imaging GRP-receptor-positive tumours, such as prostate, breast and small-cell lung cancers and gastrointestinal stromal tumours.

Experimental Section

Materials and methods: All reagents and solvents were obtained from commercial sources and used without further purification. Rink amide 4-methylbenzhydrylalanine (MBHA) resin (0.34 mmol g^{-1}; 100–200 mesh) and all of the 9-fluorenylmethoxycarbonyl (Fmoc) protected amino acids are commercially available from NovaBiochem (Laeufelfingen, Switzerland). BIM26226 was provided by Ipsen Biotech (Paris, France). ^{99m}Tc was eluted as Na[^{99m}Tc]TcO_4 from a ^{99}Mo/^{99m}Tc generator obtained from Mallinckrodt-Tyco (Petten, the Netherlands). Reactions were carried out at ambient temperature, unless otherwise noted, and were monitored by thin-layer chromatography on Merck plates precoated with silica gel 60 F-254 (0.25 mm). Spots were visualised either by UV light or iodine. Flash column chromatography was performed on silica gel 60 (Fluka). Electrospray ionisation mass spectroscopy was carried out with a Finnigan SSQ7000 apparatus (Bremen, Germany) and MALDI-MS measurements were recorded on a Voyager sSTR instrument equipped with an Nd:YAG laser (Applied Biosystems, Framingham, USA). Analytical high-performance liquid chromatography was performed on a Hewlett Packard 1050 HPLC system with a multiwavelength detector and a flow-through Berthold LB 506 Cl γ detector by using a Macherey–Nagel Nucleosil 120 C18 column. Preparative HPLC was performed on a Metrohm HPLC LC-CaDI 22–14 system with a Macherey–Nagel VP 250/21 Nucleosil 100–5 C18 column. Both analytical and preparative columns were eluted with a gradient system of mixtures of H_2O with 0.1% trifluoroacetic acid (TFA; solvent A) and acetonitrile (solvent B). Quantitative γ counting was performed with a COBRA 5003 γ-system well counter from Packard Instruments. The NMR spectra were recorded on a Bruker Avance 600 MHz spectrometer equipped with a 1.7 mm ^{1}H {^{13}C,^{15}N} CryoProbe, a Bruker DRX500 spectrometer equipped with a 5 mm ^{1}H-{^{13}C,^{15}N} CryoProbe or a Bruker DPX400 spectrometer with a 5 mm BBFO probe. Sample concentrations were approximately 8 mg in 500 μL of solvent with the 5 mm probe and 1 mg in 40 μL of solvent with the 1.7 mm probe. ^{1}H and ^{13}C NMR shifts were referenced to the solvent signals at 2.50 and 39.5 ppm, respectively. The following NMR experiments were carried out: ^{1}D–^{1}H, ^{1}D–^{13}C, ^{1}H–^{1}H COSY, ^{1}H–^{13}C COSY (HSQC) and ^{1}H–^{13}C HMBC.

6-(Hydroxy)-1,4,8,11-tetraazaundecane (01): 1,3-Dibromo-2-proponol (10 g, 46 mmol) was added dropwise to ethylenediamine (120 g, 2 moles) over a period of 1 h with vigorous stirring. The mixture was stirred at 110 °C for 24 h. Excess ethylenediamine was removed by rotary evaporation followed by high-vacuum distillation. The product was further purified by crystallisation as the hydrochloride salt. 12 M HCl (100 mL) was slowly added to a solution of the product in ethanol (250 mL) with cooling on ice. The precipitate thus formed was dissolved by addition of ethanol (150 mL) and water (50 mL) and heating of the resultant mixture to 100 °C. Additional ethanol (100 mL) was added and the solution was cooled to room temperature to obtain the tetrahydrochloride product **01** as fine white needles (10.74 g, 72%); m.p. 236–238 °C; ^{1}H NMR (D_2O): $\delta = 3.12$ (dd, 2H; CH_2), 3.25 (dd, 2H; CH_2), 3.28 (t, 2H; CH_2), 3.33 (t, 2H; CH_2), 4.34 (m, 1H; CH), 8.9 ppm (brs, 2H; NH); ^{13}C NMR (D_2O): $\delta = 35.1$, 44.5, 49.8 (2C), 62.4 ppm; MS (ESI): *m/z* (%): 177.4 (22) $[M+H]^+$, 214.1 (100) $[M+H+HCl]^+$; elemental analysis: calcd (%) for $C_7H_{20}N_4O{\cdot}4HCl$ ($0.8H_2O$): C 24.95, H 7.68, N 16.63; found: C 25.6, H 7.6, N 16.8.

***N,N′,N″,N‴*-Tetrakis(*tert*-butyloxycarbonyl)-6-(hydroxy)-1,4,8,11-tetraazaundecane (02)**: **01** (5 g, 15.6 mmol) was dissolved in water and passed through strongly basic anion exchange resin (Dowex 1; hydroxide form; 20–50 mesh). The basic fractions were collected and evaporated to dryness to obtain hydrochloride-free **01** (2.58 g, 94%).

The hydrochloride-free **01** (2.58 g, 14.6 mmol) was dissolved in DMF (25 mL) and cooled to 0 °C. A solution of di-*tert*-butyldicarbonate (16.5 mL, 72 mmol) in DMF (15 mL) was added to the mixture, followed by DIPEA (12.5 mL, 72 mmol). The reaction mixture was then stirred at room temperature for 18 h. Excess DMF was removed under vacuum and the residue was partitioned between water and ethyl acetate. The aqueous layer was extracted thrice with ethyl acetate and the combined ethyl acetate phases were washed with sodium chloride solution and dried over anhydrous sodium sulphate. Filtration and evaporation of the solvent under reduced pressure yielded **02** as a white solid (7.2 g, 86%); $R_f = 0.66$ (EtOAc:Hexane 7:3); m.p. 138–139 °C; ^{1}H NMR ([D_6]DMSO): $\delta = 1.40$ (s, 18H; CH_3), 1.42 (s, 18H; CH_3), 2.97 (dd, 2H; CH_2), 3.10 (dd, 4H; CH_2), 3.27 (dd, 4H; CH_2), 3.29 (dd, 2H; CH_2), 3.48 (m, 1H; CH), 4.67 (d, 1H; OH), 6.36 ppm (brs, 2H; NH); ^{13}C NMR ([D_6]DMSO): $\delta =$ 27.8 (6C), 27.9 (6C), 38.4 (2C), 47.4 (2C), 51.3 (2C), 68.1, 77.1 (2C), 78.1 (2C), 154.2 (2C), 154.7 ppm (2C); MS (ESI): *m/z* (%): 577.5 (100) $[M+H]^+$, 477.3 (18) $[M-C_5H_9O_2+H]^+$; elemental analysis: calcd (%) for $C_{27}H_{52}N_4O_9$: C 56.23, H 9.09, N 9.71; found: C 56.61, H 9.20, N 9.55.

***N,N′,N″,N‴*-Tetrakis(*tert*-butyloxycarbonyl)-6-(*O*-methylsulfonyl)-1,4,8,11-tetraazaundecane (03)**: Methylsulfonyl chloride (0.84 mL, 10.4 mmol) was added to a solution of **02** (3 g, 5.2 mmol) in pyridine (30 mL). The reaction mixture was stirred at room temperature until completion, as monitored by TLC. The solvent was evaporated in vacuo and the residue was taken into ethyl acetate. The organic phase was washed thrice with 10% $NaHCO_3$ and water and then dried over anhydrous sodium sulphate. Filtration and evaporation of the solvent under reduced pressure yielded the crude product, which was further purified by silica gel column chromatography with hexane and ethyl acetate (50–80%) as the eluent to obtain 2.8 g (82%) of **03** as a slightly yellow oil; $R_f = 0.58$ (Hexane:EtOAc 9:1); ^{1}H NMR ([D_6]DMSO): $\delta = 1.40$ (s, 18H; CH_3), 1.43 (s, 18H; CH_3), 3.05 (s, 3H; CH_3), 3.09 (t, 4H; CH_2), 3.17 (m, 2H; CH_2), 3.22 (m, 2H; CH_2), 3.25 (m, 2H; CH_2), 3.65 (t, 2H; CH_2), 4.60 (m, 1H; CH), 6.52 ppm (brs, 2H; NH); ^{13}C NMR ([D_6]DMSO): $\delta =$ 27.6 (6C), 27.9 (6C), 37.6 (2C), 38.3, 43.3 (2C), 46.7 (2C), 71.2, 77.3 (2C), 78.7 (2C), 154.7 (2C), 156.1 ppm (2C); MS (ESI): *m/z* (%): 655.6 (100) $[M]^+$, 656.6 (32) $[M+H]^+$, 556.5 (44) $[M-C_5H_9O_2+H]^+$.

***N,N′,N″,N‴*-Tetrakis(*tert*-butyloxycarbonyl)-6-(azido)-1,4,8,11-tetraazaundecane (04)**: A suspension of **03** (2.5 g, 3.8 mmol) and sodium azide (1 g, 15.2 mmol) in DMF (30 mL) was stirred at 75 °C for 5 h. Later, the reaction mixture was stirred at room temperature for an additional 18 h. The reaction mixture was then portioned between water and ethyl acetate. The aqueous layer was extracted with ethyl acetate and the organic phase was washed thrice with aqueous NaCl, dried (anhydrous Na_2SO_4) and filtered. The solvent was then evaporated to leave a yellow residue. This residue was subjected to silica gel column chromatography with

CH_2Cl_2 and MeOH (2–5%) to get pure **04** as a white solid (1.98 g, 88%); $R_f = 0.68$ (EtOAc:EtOH 9:1); m.p. 164–166°C; ^{1}H NMR ([D$_6$]DMSO): $\delta = 1.37$ (s, 18H; CH_3), 1.40 (s, 18H; CH_3), 3.08 (m, 4H; CH_2), 3.16 (m, 2H; CH_2), 3.21 (m, 2H; CH_2), 3.24 (m, 2H; CH_2), 3.63 (t, 2H; CH_2), 4.59 (m, 1H; CH), 6.58 ppm (brs, 2H; NH); ^{13}C NMR ([D$_6$]DMSO): $\delta =$ 28.0 (6C), 28.2 (6C), 37.7 (2C), 43.7 (2C), 47.0 (2C), 71.8, 78.0 (2C), 79.4 (2C), 155.7 (2C), 157.2 ppm (2C); HRMS (ESI): *m*/*z* calcd for $C_{27}H_{52}N_7O_8$: 602.7412 $[M+H]^+$; found: 602.7446.

***N*,*N*′,*N*″,*N*‴-Tetrakis(*tert*-butyloxycarbonyl)-6-(*O*-succinyl)-1,4,8,11-tetraazaundecane (05): 02** (250 mg, 434 μmol) was dissolved in THF (2.5 mL). Succinic anhydride (52 mg, 520 μmol) and 4-dimethylaminopyridine (53 mg, 434 μmol) were added and the mixture was stirred at room temperature overnight. TLC analysis showed a small amount of the starting material. Succinic anhydride (26 mg, 260 μmol) was again added and the mixture was stirred for an additional 6 h. The product was extracted into ethyl acetate and the organic phase was washed thrice with $NaHCO_3$ (5%) and twice with aqueous NaCl, dried (anhydrous Na_2SO_4), filtered and evaporated to get a yellow oil. Further purification by silica gel column chromatography with CH_2Cl_2 and MeOH (5%) yielded **05** as a white solid (270 mg, 92%); $R_f = 0.69$ (EtOAc:EtOH 9:1); m.p. 162–164°C; ^{1}H NMR ([D$_6$]DMSO): $\delta = 1.40$ (s, 18H; CH_3), 1.43 (s, 18H; CH_3), 2.50 (t, 2H, CH_2), 2.61 (t, 2H, CH_2), 3.12 (m, 4H; CH_2), 3.16 (t, 2H; CH_2), 3.22 (m, 2H; CH_2), 3.27 (m, 2H; CH_2), 3.65 (t, 2H; CH_2), 5.11 (m, 1H; CH), 6.62 (brs, 2H; NH), 12.38 ppm (brs, 1H, COOH); ^{13}C NMR ([D$_6$]DMSO): $\delta = 28.2$ (6C), 28.4 (6C), 29.5, 31.9, 38.1 (2C), 48.2 (2C), 49.8 (2C), 72.6, 79.2 (2C), 79.8 (2C), 154.1 (2C), 155.9 (2C), 173.1, 176.8 ppm; MS (ESI): *m*/*z* (%): 677.6 (100) $[M+H]^+$, 699.8 (26) $[M+Na]^+$.

***N*,*N*′,*N*″,*N*‴-Tetrakis(*tert*-butyloxycarbonyl)-6-(carboxy)-1,4,8,11-tetraazaundecane (06)**: A solution of 3-bromo-2-(bromomethyl)propionic acid (1 g, 4 mmol) in THF (10 mL) was added drop by drop to ethylenediamine (10.7 mL, 0.16 mol) in THF (100 mL) with vigorous stirring. The reaction mixture was stirred at room temperature and the excess solvent and ethylenediamine were evaporated under reduced pressure. The concentrated residue was dissolved in a mixture of dioxane (24 mL), water (12 mL) and 1N NaOH (12 mL) and cooled to 4°C. Di-*tert*-butyl dicarbonate (4.4 g, 20 mmol) was added slowly to this reaction mixture with stirring. The stirring was continued for 1 h at room temperature and the mixture was then concentrated in vacuo to a volume of about 15–20 mL. The concentrated residue was cooled in an ice-water bath, covered with a layer of ethyl acetate (50 mL) and acidified with cold 1N HCl (15 mL). The aqueous phase was immediately extracted with ethyl acetate (3× 50 mL). The ethyl acetate extracts were pooled, washed with water, dried (anhydrous Na_2SO_4), filtered and evaporated in vacuo. The crude product thus obtained was further purified by silica gel column chromatography with ethyl acetate and ethanol (5–8%) to get **06** as a white solid (1.5 g, 62%); $R_f = 0.76$ (EtOAc:EtOH 9:1); m.p. 153–154°C; ^{1}H NMR ([D$_6$]DMSO): $\delta = 1.40$ (s, 18H; CH_3), 1.42 (s, 18H; CH_3), 2.92 (m, 1H; CH), 3.07 (t, 4H; CH_2), 3.15 (m, 2H; CH_2), 3.25 (m, 2H; CH_2), 3.30 (t, 4H; CH_2), 6.39 (brs, 2H; NH), 12.42 ppm (brs, 1H, COOH); ^{13}C NMR ([D$_6$]DMSO): $\delta = 27.7$ (6C), 27.9 (6C), 38.2 (2C), 44.1, 46.8 (2C), 47.2 (2C), 77.1 (2C), 78.4 (2C), 153.9 (2C), 154.6 (2C), 173.3 ppm; MS (ESI): *m*/*z* (%): 605.5 (100) $[M+H]^+$, 627.4 (12) $[M+Na]^+$; elemental analysis: calcd (%) for $C_{28}H_{53}N_4O_{10}$: C 55.61, H 8.67, N 9.26; found: C 54.93, H 8.26, N 8.86.

Peptide synthesis: The solid-phase peptide synthesis was performed on a semiautomatic peptide synthesiser (RinkCombichem, Bubendorf, Switzerland) by employing the standard Fmoc strategy.[45] The peptide amide, D-Phe-Gln-Trp-Ala-Val-Gly-His-Sta-Leu-NH_2, was assembled on Rink amide MBHA resin. Triphenylmethyl (Trt) was used as the protecting group for Gln, Asn and His and Boc was used to protect Trp. The coupling reactions were achieved with a threefold excess of the Fmoc-protected amino acids, by using diisopropylcarbodiimide (DIC)/1-hydroxy-1*H*-benzotriazole (HOBt) as the activating agents in DMF/*N*-methylpyrrolidine (NMP). After a coupling time of 2 h, the completion of the reaction was monitored by a standard Kaiser test. Fmoc removal was achieved with 20% piperidine in DMF in 3 successive 10 min treatments. A spacer was introduced by consecutive coupling of Fmoc-Gly-OH and Fmoc-4-aminobenzoic acid by using HATU as the activating agent.

Synthesis of N4-BB-ANT: After assembly of the desired amino acids on the resin, the final Fmoc group was removed. The tetraamine-chelator precursor **06** (3 equiv) was coupled to the N terminal of the peptides by using HATU (3.3 equiv) and DIPEA (7 equiv) for 3 h. The cleavage of the peptide–chelator conjugate from the resin and simultaneous side-chain deprotection was accomplished by incubation for 2.5 h in a cleavage cocktail comprising TFA:thioanisole:H_2O:triisopropylsilane (95:3:1:1). The resin was then filtered and washed with the above mixture; evaporation of the filtrate was followed by trituration with diethyl ether, which yielded the crude product. The crude conjugate was further purified by semi-preparative HPLC (0 min, 80% A, 20 min 50% A) to obtain N4-BB-ANT with purity of >97%; $R_t = 18.74$ min (analytical RP-HPLC; 0 min, 95% A; 30 min 50% A); MS (ESI): *m*/*z* (%): 1476.1 (16) $[M+H]^+$, 738.4 (100) $[M+H]^{2+}$.

Radiolabelling: The labelling of N4-BB-ANT with ^{99m}Tc was achieved by following the protocol described earlier.[27] Briefly, a stock solution of N4-BB-ANT (1 mM) was prepared by dissolving it in a mixture (8:2 *v*/*v*) of acetic acid (50 mM) and ethanol. A mixture of 0.5M phosphate buffer (pH 11.5; 50 μL) and 0.1M sodium citrate (5 μL) was taken up in an Eppendorf pipette. Na[^{99m}Tc]TcO_4 generator eluate (18–20 mCi, 700 μL), N4-BB-ANT solution (20 nmol, 20 μL) and freshly prepared $SnCl_2$ solution in ethanol (25 μg, 25 μL) were added to this mixture. The reaction mixture was incubated at room temperature for 30 min. Quality control was performed by analytical RP-HPLC.

Cell lines: Human embryonic kidney 293 (HEK293) cells that stably express the HA-epitope-tagged human GRP receptor (HEK-GRPr cells) were generated as previously described[24,28] and cultured at 37°C and 5% CO_2 in Dulbecco's modified Eagle's medium (DMEM) with GlutaMAX-I containing 10% (*v*/*v*) fetal bovine serum (FBS), 100 U mL^{-1} penicillin, 100 μg mL^{-1} streptomycin and 750 μg mL^{-1} G418. Human prostate cancer (PC3) cells were obtained from the American Type Culture Collection (Virginia, USA) and cultured at 37°C and 5% CO_2 in DMEM containing 2 mM L-glutamine and supplemented with 10% (*v*/*v*) FBS, 100 U mL^{-1} penicillin and 100 μg mL^{-1} streptomycin. All culture reagents were from Invitrogen (Basel, Switzerland) or from BioConcept (Allschwil, Switzerland).

Receptor-binding-affinity measurements: IC_{50} values were determined by in vitro GRP-receptor autoradiography on cryostat sections of well-characterised prostate carcinomas, as described previously.[46] The radioligand used was [^{125}I–Tyr4]-bombesin, which is known to preferentially label GRP receptors.[47]

Immunofluorescence-based internalisation assay: The immunofluorescence microscopy-based internalisation assay for GRP receptors with HEK-GRPr cells was performed as previously described.[28] Briefly, HEK-GRPr cells were grown on poly-D-lysine coated (20 μg mL^{-1}; Sigma–Aldrich, St. Louis, MO) 35 mm 4-well plates (Cellstar, Greiner Bio-One GmbH, Frickenhausen, Germany). Cells were treated either with 10 nmol L^{-1} bombesin, with 1 μmol L^{-1} N4-BB-ANT or, to evaluate potential antagonism, with 10 nmol L^{-1} bombesin in the presence of a 100-fold excess of N4-BB-ANT for 30 min at 37°C and 5% CO_2 in growth medium. Cells were then processed for immunofluorescence microscopy by using the mouse monoclonal HA-epitope antibody at a dilution of 1:1000 as the first antibody (Covance, Berkeley, CA) and Alexa Fluor 488 goat anti-mouse immunoglobulin G (IgG; H+L) at a dilution of 1:600 as the secondary antibody (Molecular Probes, Eugene, OR). The cells were imaged by using a Leica DM RB immunofluorescence microscope and an Olympus DP10 camera.

Calcium mobilisation assay: Intracellular calcium mobilisation was measured in PC3 cells by using the Calcium 3 Assay kit (Molecular Probes, Inc.) following the protocol described earlier with slight modifications.[22] In brief, PC3 cells (25000 cells per well) were seeded in 96-well plates and cultured for 1 d at 37°C and 5% CO_2. On the day of the experiment, the medium was removed and the cells were then loaded with 100 μL per well of Ca dye in assay buffer (Hank's balanced salt solution (HBSS) and 20 mM 2-[4-(2-hydroxyethyl)-1-piperazinyl]ethanesulfonic acid (HEPES)) containing 2.5 mM probenecid for 1 h at 37°C. The agonist Tyr^4-bombesin

was diluted in a dilution buffer (HBSS with 20 mM HEPES, 0.1 % bovine serum albumin (BSA), 0.05 % pluronic acid) to a concentration of 100 nM and dispensed into a reagent-source 96-well plate. Various concentrations of antagonists (N4-BB-ANT, RM1, BIM26226) ranging from 0.1 nM to 100 μM were prepared in the dilution buffer and loaded into the same 96-well plate. Cell- and peptide-containing plates were loaded into a FLEX station 3 Microplate Reader (Molecular Devices). Intracellular calcium mobilisation was recorded at room temperature for 4 min by monitoring of fluorescence emission at 525 nm (with $\lambda_{ex} = 485$ nm) and the data were analysed by SoftMax Pro software (Molecular Devices). The instrument was programmed so that the antagonist (20 μL at various concentrations) was added to cell plates and preincubated for 1 min prior to addition of the agonist (20 μL).

Receptor-mediated cellular-uptake kinetics: The PC3 cells were seeded at a density of 0.8–1.1 million cells per well in 6-well plates and incubated overnight with internalisation buffer (DMEM, 1 % FBS, amino acids and vitamins; pH 7.4) to obtain good cell adherence. On the day of the experiment, cells were washed once with internalisation buffer (2 mL) and incubated with fresh medium (1.3 mL) for 1 h at 37 °C. Approximately 6 kBq (0.25 pmol) of ^{99m}Tc-N4-BB-ANT per well was added and the cells were incubated at 37 °C for the indicated time periods in triplicate. To determine non-specific membrane binding and internalisation, cells were incubated with radioligand in the presence of a 1000-fold excess of blocking agent (BIM26226). The plates were removed at different time points (0.5, 1, 2 and 4 h) and the cellular uptake was stopped by removing medium from the cells and by washing twice with ice-cold PBS (1 mL). An acid wash for 5 min with a glycine buffer (pH 2.8) on ice was also performed twice. This procedure was performed to distinguish between membrane-bound (acid-releasable) and internalised (acid-resistant) radiopeptide. Finally, the cells were treated with 1 N NaOH. The culture medium, the receptor-bound fraction and the internalised fraction were measured radiometrically in a γ counter (Cobra II).

Fate of receptor-bound radioligand: The PC3 cells were prepared in 6-well plates as described above. On the day of the experiment, cells were washed once with internalisation buffer (2 mL) and incubated with fresh medium (1.3 mL) for 1 h at 37 °C. Later, the plates were placed on ice for 30 min. A 1000-fold excess of blocking agent was added to selected wells to determine non-specific binding. ^{99m}Tc-N4-BB-ANT (0.25 pmol, 6 kBq) was added to each well and allowed to bind to the cells at 4 °C. After 2 h of incubation, the cells were quickly washed twice with ice-cold PBS and fresh pre-warmed (37 °C) culture medium (1 mL) was added to each well. This was followed by incubation at 37 °C and 5 % CO_2. The plates were removed at different time points (10, 20 and 30 min, 1, 2 and 4 h) and treated as above.

Biodistribution and imaging studies in PC3 tumour-bearing nude mice: Animals were kept, treated, and cared for in compliance with the guidelines of the Swiss regulations (approval 789). Female nude mice were implanted subcutaneously with 10–12 million PC3 tumour cells, which were freshly expanded in sterilised PBS (pH 7.4). 11 days after inoculation, the mice showed solid palpable tumour masses (tumour weight: 60–180 mg) and were used for the experiments. The mice were injected in the tail vein with ^{99m}Tc-N4-BB-ANT (10 pmol; about 0.37 MBq) in NaCl solution (0.1 mL; 0.9 % with 0.1 % BSA). The mice were sacrificed under anaesthesia at 1, 4 and 24 h post injection (in groups of 4–6 mice per time point). Organs of interest and blood were collected, rinsed of excess blood, blotted dry, weighed and counted in a γ counter. For the determination of non-specific uptake in the tumour or receptor-positive organs, a group of 4 animals was pre-injected with a 2000-fold excess of cold N4-BB-ANT in 0.9 % NaCl solution (0.1 mL); after 5 min, the radiolabelled peptide was injected. The percentage of injected activity per gram (% IA g^{-1}) was calculated for each tissue. The total counts injected per animal were determined by extrapolation from counts of an aliquot taken from the injected solution as a standard.

Two mice were used for SPECT/CT imaging. The mice were injected with ^{99m}Tc-N4-BB-ANT (200 pmol; approximately 15 MBq). For blocking purposes, one mouse was pre-injected with N4-BB-ANT (0.2 μmol) 5 min before injection of the radiolabelled peptide. The mice were anaesthetised 12 h after injection and images were acquired by using a clinical SPECT/CT camera (Symbia T2, Siemens, Germany). The SPECT images were reconstructed iteratively (4 subsets, 8 iterations) and automatically fused with three-dimensional reconstructed images from the CT (2× 1.25 mm slices, 130 kV, 48 mAs).

Statistical methods: Student's T test was used to determine statistical significance. Differences at the 95 % confidence level ($P < 0.05$) were considered significant.

Acknowledgements

This work was supported by the Swiss Cancer League (grant no. OCS-01778-08-2005), the Swiss National Science Foundation (grant no. 320000-118333) and Bayer Schering Pharma, Germany. We thank Sibylle Tschumi and Pia Powell for expert technical assistance, Ingo Muckenschnabel (Novartis Pharma) for HRMS and the Department of Chemistry, University of Basel, for elemental analysis.

[1] S. M. Ametamey, S. M. Honer, P. A. Schubiger, *Chem. Rev.* **2008**, *108*, 1501–1516.
[2] P. Blower, *Dalton Trans.* **2006**, 1705–1711.
[3] R. Alberto, *Top. Curr. Chem.* **2005**, *252*, 1–44.
[4] E. Garcia-Garayoa, R. Schibli, P. A. Schubiger, *Nucl. Sci. Tech.* **2007**, *18*, 88–100.
[5] V. Maes, E. Garcia-Garayoa, P. Blauenstein, D. Tourwe, *J. Med. Chem.* **2006**, *49*, 1833–1836.
[6] M. J. Abrams, M. Juweid, C. I. tenKate, D. A. Schwartz, M. M. Hauser, F. E. Gaul, A. J. Fuccello, R. H. Rubin, H. W. Strauss, A. J. Fischman, *J. Nucl. Med.* **1990**, *31*, 2022–2028.
[7] J. W. Babich, H. Solomon, M. C. Pike, D. Kroon, W. Graham, M. J. Abrams, R. G. Tompkins, R. H. Rubin, A. J. Fischman, *J. Nucl. Med.* **1993**, *34*, 1964–1974.
[8] A. J. Fischman, D. Rauh, H. Solomon, J. W. Babich, R. G. Tompkins, D. Kroon, H. W. Strauss, R. H. Rubin, *J. Nucl. Med.* **1993**, *34*, 2130–2134.
[9] R. C. M. King, B.-U. Surfraz, S. C. G. Biagini, P. J. Blower, S. J. Mather, *Dalton Trans.* **2007**, 4998–5007.
[10] E. von Guggenberg, M. Behe, T. M. Behr, M. Saurer, T. Seppi, C. Decristoforo, *Bioconjugate Chem.* **2004**, *15*, 864–871.
[11] D. Storch, M. Behe, M. A. Walter, J. Chen, P. Powell, R. Mikolajczak, H. R. Maecke, *J. Nucl. Med.* **2005**, *46*, 1561–1569.
[12] C. Decristoforo, S. J. Mather, W. Cholewinski, E. Donnemiller, G. Riccabona, R. Moncayo, *Eur. J. Nucl. Med.* **2000**, *27*, 1318–1325.
[13] J. B. Cwikla, R. Mikolajczak, D. Pawlak, J. R. Buscombe, A. Nasierowska-Guttmejer, A. Bator, H. R. Maecke, J. Walecki, *J. Nucl. Med.* **2008**, *49*, 1060–1065.
[14] A. Hubalewska-Dydejczyk, K. Fross-Baron, R. Mikolajczak, H. R. Maecke, B. Huszno, D. Pach, A. Sowa-Staszczak, B. Janota, P. Szybinski, J. Kulig, *Eur. J. Nucl. Med. Mol. Imaging* **2006**, *33*, 1123–1133.
[15] T. Maina, B. Stolz, R. Albert, C. Bruns, P. Koch, H. Macke, *Eur. J. Nucl. Med.* **1994**, *21*, 437–444.
[16] P. Koch, H. Maecke, *Angew. Chem.* **1992**, *104*, 1492–1494; *Angew. Chem. Int. Ed. Engl.* **1992**, *31*, 1507–1509.
[17] D. Eshima, A. Taylor, Jr., A. R. Fritzberg, S. Kasina, L. Hansen, J. F. Sorenson, *J. Nucl. Med.* **1987**, *28*, 1180–1186.
[18] H. P. Vanbilloen, G. M. Bormans, M. J. De Roo, A. M. Verbruggen, *Nucl. Med. Biol.* **1995**, *22*, 325–338.
[19] S. Liu, D. S. Edwards, R. J. Looby, M. J. Poirier, M. Rajopadhye, J. P. Bourque, T. R. Carroll, *Bioconjugate Chem.* **1996**, *7*, 196–202.
[20] T. Rao, D. Adhikesavalu, A. Camerman, A. R. Fritzberg, *J. Am. Chem. Soc.* **1990**, *112*, 5798–5804.
[21] S. Z. Lever, K. E. Baidoo, A. Mahmood, *Inorg. Chim. Acta* **1990**, *176*, 183–184.
[22] S. K. Meegalla, K. Plossl, M. P. Kung, S. Chumpradit, D. A. Stevenson, S. A. Kushner, W. T. McElgin, P. D. Mozley, H. F. Kung, *J. Med. Chem.* **1997**, *40*, 9–17.

[23] H. F. Kung, Y. Z. Guo, C. C. Yu, J. Billings, V. Subramanyam, J. C. Calabrese, *J. Med. Chem.* **1989**, *32*, 433–437.
[24] R. H. Mach, H. F. Kung, Y. Z. Guo, C. C. Yu, V. Subramanyam, J. C. Calabrese, *Int. J. Rad. Appl. Instrum. B* **1989**, *16*, 829–837.
[25] S. Meegalla, K. Plossl, M. P. Kung, S. Chumpradit, D. A. Stevenson, D. Frederick, H. F. Kung, *Bioconjugate Chem.* **1996**, *7*, 421–429.
[26] J. P. O'Neil, S. R. Wilson, J. A. Katzenellenbogen, *Inorg. Chem.* **1994**, *33*, 319–323.
[27] M. L. Thakur, H. Kolan, J. Li, R. Wiaderkiewicz, V. R. Pallela, R. Duggaraju, A. V. Schally, *Nucl. Med. Biol.* **1997**, *24*, 105–113.
[28] R. Cescato, T. Maina, B. Nock, A. Nikolopoulou, D. Charalambidis, V. Piccand, J. C. Reubi, *J. Nucl. Med.* **2008**, *49*, 318–326.
[29] T. Maina, B. Nock, A. Nikolopoulou, P. Sotiriou, G. Loudos, D. Maintas, P. Cordopatis, E. Chiotellis, *Eur. J. Nucl. Med. Mol. Imaging* **2002**, *29*, 742–753.
[30] B. A. Nock, A. Nikolopoulou, A. Galanis, P. Cordopatis, B. Waser, J. C. Reubi, T. Maina, *J. Med. Chem.* **2005**, *48*, 100–110.
[31] B. Nock, A. Nikolopoulou, E. Chiotellis, G. Loudos, D. Maintas, J. C. Reubi, T. Maina, *Eur. J. Nucl. Med.* **2003**, *30*, 247–258.
[32] B. Nock, P. Koch, F. Evard, G. Paganelli, H. Maecke in *$^{99m}TcN_4$–Lys–biotin, a new biotin derivative useful for pretargeted avidin–biotin immunoscintigraphy: synthesis, evaluation and comparison with other ^{99m}Tc–biotin conjugates, Vol. 4* (Eds.: M. Nicolini, G. Bandoli, U. Mazzi), SGE Ditoriali, Padua, **1995**, pp. 429–432.
[33] C. Decristoforo, T. Maina, B. Nock, M. Gabriel, P. Cordopatis, R. Moncayo, *Eur. J. Nucl. Med. Mol. Imaging* **2003**, *30*, 1211–1219.
[34] B. A. Nock, T. Maina, M. Behe, A. Nikolopoulou, M. Gotthardt, J. S. Schmitt, T. M. Behr, H. R. Macke, *J. Nucl. Med.* **2005**, *46*, 1727–1736.
[35] L. E. Lantry, E. Cappelletti, M. E. Maddalena, J. S. Fox, W. Feng, J. Chen, R. Thomas, S. M. Eaton, N. J. Bogdan, T. Arunachalam, J. C. Reubi, N. Raju, E. C. Metcalfe, L. Lattuada, K. E. Linder, R. E. Swenson, M. F. Tweedle, A. D. Nunn, *J. Nucl. Med.* **2006**, *47*, 1144–1152.
[36] J. C. Reubi, *Endocr. Rev.* **2003**, *24*, 389–427.
[37] M. Ginj, H. Zhang, B. Waser, R. Cescato, D. Wild, X. Wang, J. Erchegyi, J. Rivier, H. R. Maecke, J. C. Reubi, *Proc. Natl. Acad. Sci. USA* **2006**, *103*, 16436–16441.
[38] R. Mansi, X. Wang, F. Forrer, S. Kneifel, M. L. Tamma, B. Waser, R. Cescato, J. C. Reubi, H. R. Maecke, *Clin. Cancer Res.* **2009**, *15*, 5240–5249.
[39] J. Prescher, C. Bertozzi, *Nat. Chem. Biol.* **2005**, *1*, 13–21.
[40] C. D. Hein, X. M. Liu, D. Wang, *Pharm. Res.* **2008**, *25*, 2216–2230.
[41] V. V. Rostovtsev, L. G. Green, V. V. Fokin, K. B. Sharpless, *Angew. Chem.* **2002**, *114*, 2708–2711; *Angew. Chem. Int. Ed.* **2002**, *41*, 2596–2599.
[42] C. W. Tornoe, C. Christensen, M. Meldal, *J. Org. Chem.* **2002**, *67*, 3057–3064.
[43] D. H. Coy, Z. Mungan, W. J. Rossowski, B. L. Cheng, J. T. Lin, J. E. Mrozinski, Jr., R. T. Jensen, *Peptides* **1992**, *13*, 775–781.
[44] H. Zhang, PhD thesis, Basel University (Switzerland), **2005**; http://edoc.unibas.ch/diss/DissB_7877.
[45] E. Atherton, R. Sheppard in *Fluorenylmethoxycarbonyl-polyamide solid phase peptide synthesis. General principles and development*, Oxford Information Press, Oxford, **1989**, pp. 25–38.
[46] R. Markwalder, J. C. Reubi, *Cancer Res.* **1999**, *59*, 1152–1159.
[47] S. R. Vigna, C. R. Mantyh, A. S. Giraud, A. H. Soll, J. H. Walsh, P. W. Mantyh, *Gastroenterology* **1987**, *93*, 1287–1295.

Received: July 20, 2009
Revised: November 24, 2009
Published online: January 11, 2010

